

Cite this: DOI: 00.0000/xxxxxxxxxx

Structural and dynamical impact of water dilution on egg yolk properties - *Supplementary Information*[†]

Floriane Gerony,^{a,b} Agathe Fanost,^{a,b} Zlansu R. Tan,^a Natalie Malikova,^a Laurent Michot,^a Marie Poirier-Quinot,^c Laurence de Viguerie,^b Maguy Jaber,^b Guillaume Mériguet,^a and Anne-Laure Rollet^{*a}

Received Date
Accepted Date

DOI: 00.0000/xxxxxxxxxx

Contents

1 SAXS	1
1.1 EY diluted in linseed oil	1
1.2 Comparison with LDL of human serum.	2
2 NMR spectroscopy	2
3 Rheology	3
4 NMR relaxometry	3
5 pH evolution upon water dilution	4

1 SAXS

To help to decipher the different features observed in the SAXS curve of EY, two comparisons have been carried out. The first one concerns mixtures of EY and linseed oil. The second one concerns LDL from human serum, for which several publications have reported detailed investigations.

1.1 EY diluted in linseed oil

The SAXS patterns of EY/linseed oil mixtures from pure EY to pure oil are displayed in Fig. S1. By increasing the amount of linseed oil, the SAXS curves are modified only above 0.2 \AA^{-1} . More precisely, one notes the increase of the peak at 1.38 \AA^{-1} , that allows us to attribute it to the fatty acids contained in the LDL.

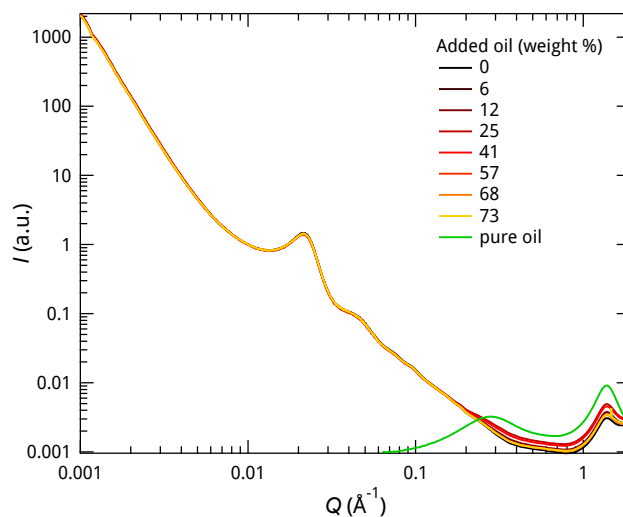


Fig. S1 Small angle X-ray scattering (SAXS) signal of a series of egg yolk samples, with increasing mass % of linseed oil.

^a Laboratoire PHysico-chimie des Électrolytes et Nanosystèmes Interfaciaux (PHENIX), Sorbonne Université/CNRS 4 place Jussieu, F-75005 Paris (France); E-mail: anne-laure.rollet@sorbonne-universite.fr

^b Laboratoire d'Archéologie Moléculaire et Structurale (LAMS), Sorbonne Université/CNRS, 4 place Jussieu, F-75005 Paris (France), France

^c Université Paris-Saclay, CNRS, Inserm, Laboratoire d'Imagerie Biomédicale Multimodale Paris Saclay, Orsay 91401, France

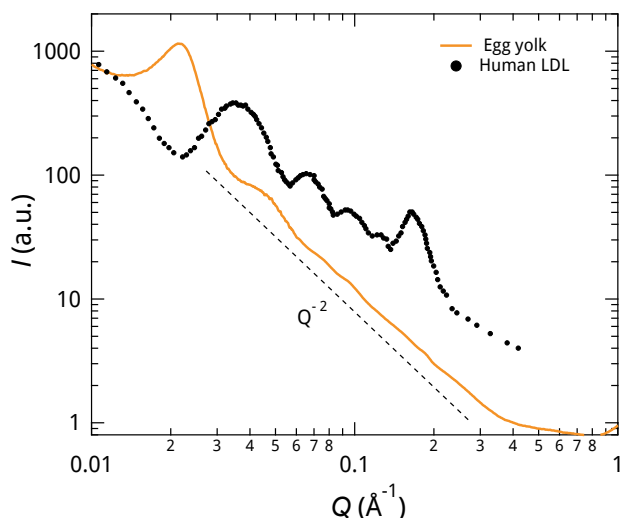


Fig. S2 Small angle X-ray scattering (SAXS) of EY and of LDL of human serum extracted from ref¹. The curves have been shifted in intensity in order to better see the features of each curve.

1.2 Comparison with LDL of human serum.

The SAXS curves of LDL of human serum and of EY have been plotted on the same figure for comparison (Fig. S2). The resemblance is not obvious, though two clear peaks at roughly 0.037 and 0.065 Å⁻¹, plus two weak peaks around 0.095 and 0.12 Å⁻¹ are present. They fall at higher Q value, consistently with the smaller size of the human LDL (about 12 nm) than the EY one. The peak around 0.21 Å⁻¹ in SAXS curve of LDL of human serum is completely absent in EY one. In addition, while the four first peaks in EY lay on a Q^{-2} dependence, those in LDL of human serum lay on $Q^{-\beta}$ with clearly $\beta < -2$.

The human LDL SAXS curves were successfully modelled in the literature using only the form factor (form of the scattering object) without considering the structure factor (spatial distribution of the scattering objects)¹. The human LDL can be described as core-shell flattened spheres. Using a similar form factor for EY does not allow us to fit the experimental data. This fact is explained by a crucial difference between the two series of SAXS curves. First, the Q dependence is -2 for EY and lower for LDL of human serum. Second, a clearly depression is observed before the first peak at 0.037 Å⁻¹ in human serum LDL curves, whereas it is completely absent before the first peak at 0.022 Å⁻¹ in EY curve. It shows the presence of the structure factor overlying the form factor peak. This is supported by the position evolution of the peak during the first steps of dilution, that is compatible with a weak repulsive interaction between the scatterers close to a hard sphere one. Stronger repulsion would lead to a significative change of the peak position with dilution while sticky interaction would give rise to some aggregation features absent in the SAXS data. From this conclusion, the opposite variation of the position of the second peak around 0.048 Å⁻¹ upon water dilution does not appear surprising anymore. Contrary to the first peak, this second peak is not affected by the shift of the structure factor peak, and its evolution is only due to a change in size and/or

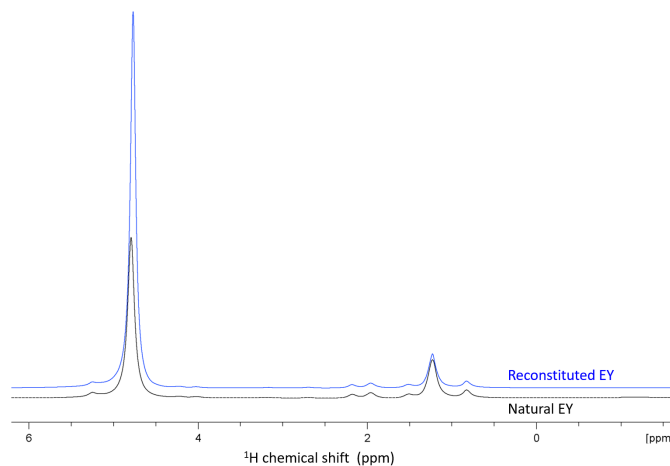


Fig. S3 ¹H NMR spectra of *tempera* solutions made with reconstituted EY (blue) and natural EY (black) recorded at 300 MHz.

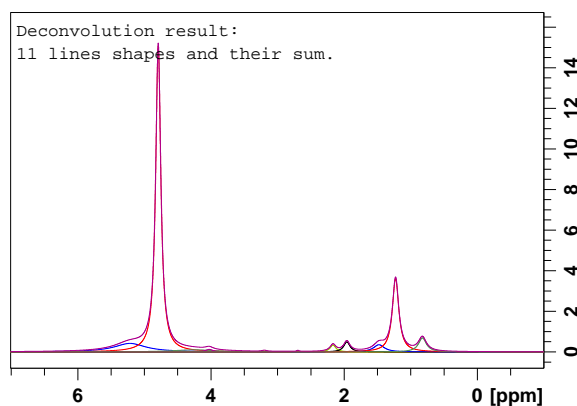


Fig. S4 NMR spectrum of egg yolk + 1 ml of water (*tempera* recipe).

shape of the LDL.

2 NMR spectroscopy

Reconstituted EY was not the matter of the present study and is just a help in some part of the NMRD analysis. Consequently, its characterization was not fully carried out. The initial objective was to use reconstituted EY instead of natural EY in the various studies about *tempera* in order to reduce the variability coming from natural EY purchase. The reproducibility of natural EY we observed with different techniques on one hand and on the requirement of adding two times more water to reconstituted EY than present in natural EY on the other hand, show that the use of reconstituted EY for the study of *tempera* paint is not appropriate. Nevertheless, the NMR spectrum of reconstituted EY has been recorded and compared to the one of natural EY (Fig. S3). Both can be superimposed.

The NMR spectrum of *tempera* solution with 7.1 wt% added water has been recorded at 300 MHz (figure S4). The deconvolution of the different peaks and their integration has been carried out on Topspin Bruker software.

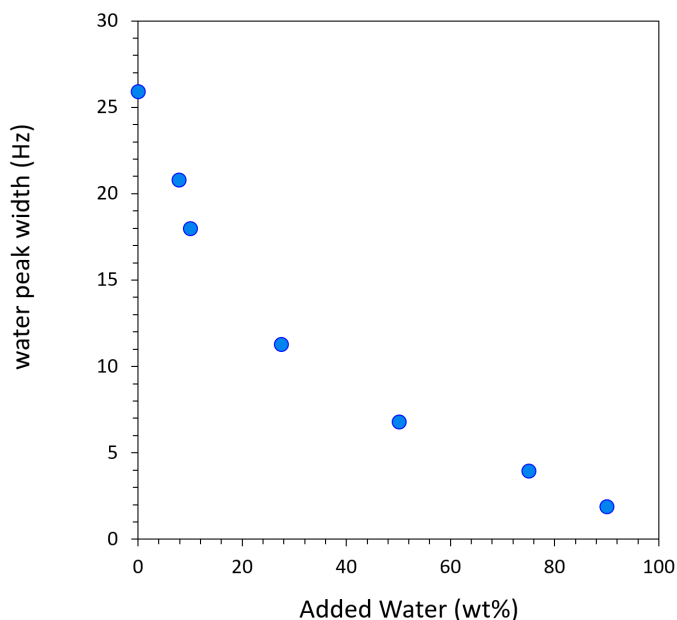


Fig. S5 ^1H NMR linewidth at 62 MHz of the water peak as a function of added water.

3 Rheology

The values of the EY/water mixtures relative viscosity, i.e. η/η_0 have been compared to the theoretical values of Pal's model². In equation 1, we use the two possible extrema for the maximum volume fraction that are for glass ($\phi_m = 0.58$) and for hexagonal compact packing hcp ($\phi_m = 0.74$). In both cases, the calculated values are much lower than the values for EY/water mixtures, showing that interactions occur between LDL probably mediated by the proteins at their surface.

$$\eta_r = \left(1 - \left[1 + \frac{1 - \phi_m}{\phi_m^2} \phi \right] \phi \right)^{-2.5} \quad (1)$$

4 NMR relaxometry

The NMRD profile for reconstituted EY is shown in figure S7 and compared with the one for natural EY. The higher R_1 component NMRD profile (i.e. higher R_1) for reconstituted EY is parallel to the one for natural EY but is lower about a factor 2. It is related to the fact that more water than normally present in EY (about a factor 2) should be added to the dry EY powder to obtain a proper viscosity. Adding just the water amount of natural EY, i.e. 50%, yields a granular paste. It can be recalled that reconstituted EY is not obtained just by lyophilization, but also is mildly heated (61°C) for pasteurization. The lower R_1 component NMRD profile for reconstituted EY is difficult to extract and is therefore very noisy.

Fig. S8 displays the NMRD dispersion profiles of lyophilised EY and reconstituted EY dispersed again in D_2O (99.96%). All the profiles are superimposed and resemble the NMRD dispersion profile of FA.

Fig. S9 shows that relaxation dispersion profiles of the water component superimpose fairly when rescaled by dividing by the

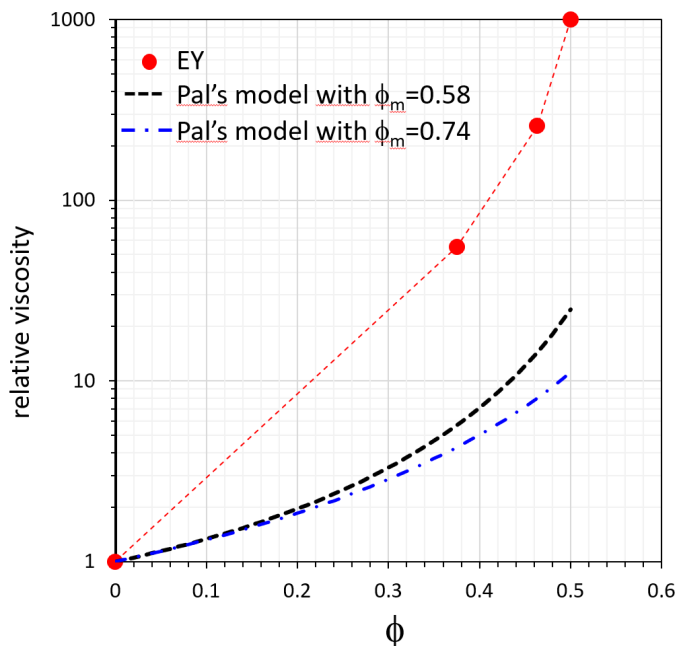


Fig. S6 Comparison of the relative viscosity of EY/water mixtures and the values calculated using Pal's model for thickened emulsions.

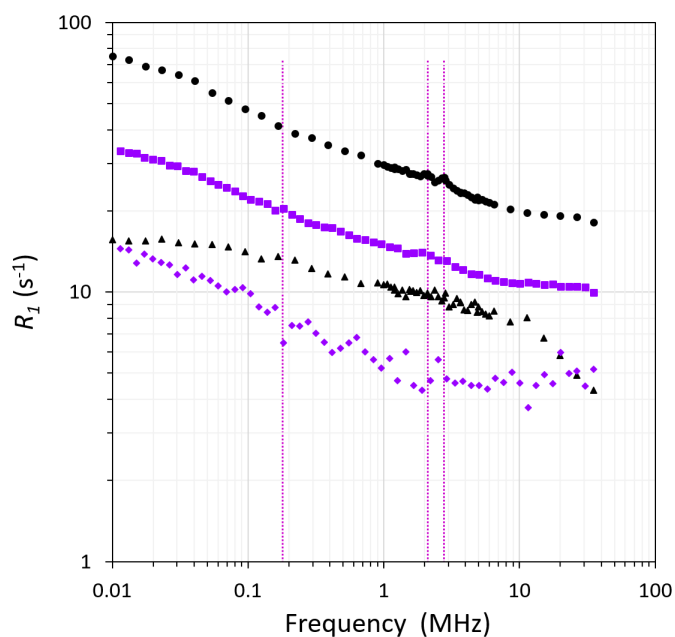


Fig. S7 NMRD Profiles for reconstituted EY ($R_{1\text{water}}$ purple square and $R_{1\text{FA}}$ purple diamond) and for natural EY ($R_{1\text{water}}$ black circle and $R_{1\text{FA}}$ black triangle).

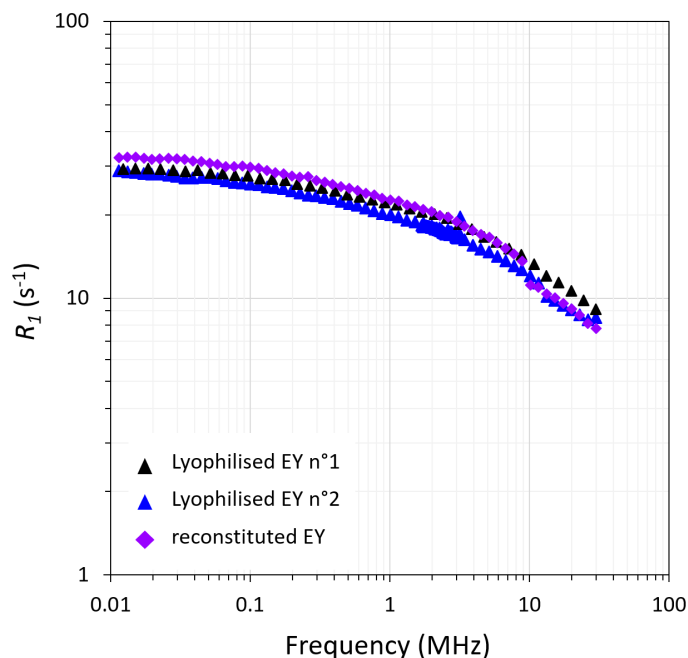


Fig. S8 NMRD profiles of two lyophilised natural EY coming from different purchases (black and blue) and of reconstituted EY (purple) dispersed in D₂O.

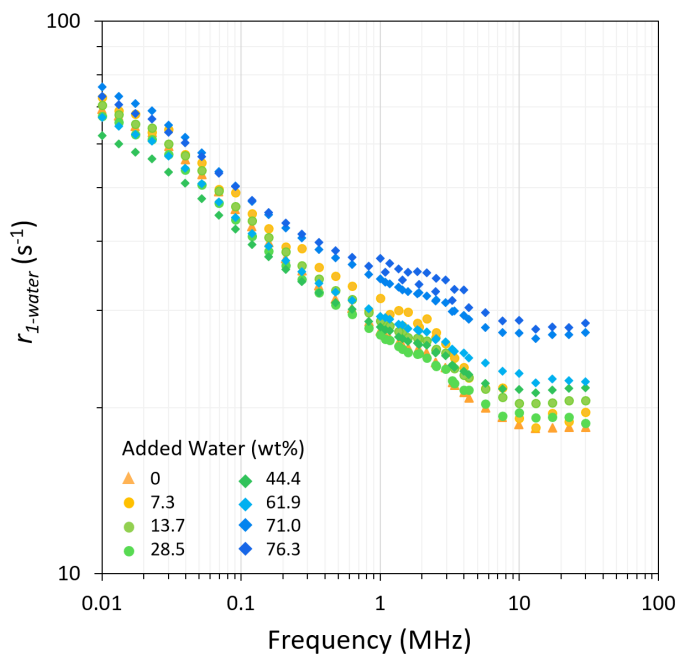


Fig. S9 NMRD Profiles of the water component normalized by dividing with $\phi_v/(1 - \phi_v)$.

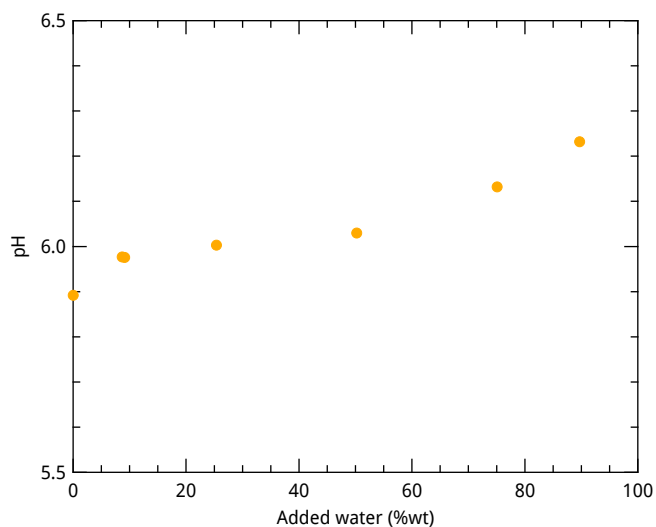


Fig. S10 Evolution of the pH during the dilution of the yolk with water.

volume fraction. This is not exactly the case when the water and FA component of the relaxation cannot be distinguished when too close (dilute samples).

5 pH evolution upon water dilution

The pH of the tempera solution has been measured as a function of the amount of added water (Figure S10). The pH increases slightly between 5.9 in pure natural EY and 6.25 in EY + 90 wt% added water. It can be noticed that the evolution is not monotonous after a first increase from 5.9 to 6 (10 wt%), pH is stable up to 50 wt%, due to buffering effect.

Notes and references

- 1 S. Maric, T. K. Lind, J. Lyngsø, M. Cárdenas and J. S. Pedersen, Modeling Small-Angle X-ray Scattering Data for Low-Density Lipoproteins: Insights into the Fatty Core Packing and Phase Transition, *ACS Nano*, 2017, **11**, 1080–1090.
- 2 R. Pal, New Generalized Viscosity Model for Non-Colloidal Suspensions and Emulsions, *Fluids*, 2020, **5**, 150.